Dissipative dispersion-managed solitons in mode-locked lasers

Brandon G. Bale,* Sonia Boscolo, and Sergei K. Turitsyn

Photonics Research Group, School of Engineering and Applied Science, Aston University, Birmingham B4 7ET, UK

**Corresponding author: b.bale@aston.ac.uk*

Received May 20, 2009; revised August 6, 2009; accepted September 9, 2009; posted October 5, 2009 (Doc. ID 111449); published October 22, 2009

We extend the theory of dispersion-managed solitons to dissipative systems with a focus on mode-locked fiber lasers. Dissipative structures exist at high map strengths, leading to the generation of stable, short pulses with high energy. Two types of intramap pulse evolution are observed depending on the net cavity dispersion. These are characterized by a reduced model, and semianalytical solutions are obtained. © 2009 Optical Society of America

OCIS codes: 140.4050, 140.3538.

Over the past two decades, mode-locked lasers have evolved from fundamental science to commercial instruments, with a wide variety of applications [1]. The most important processes in a passively mode-locked laser are linear group velocity dispersion (GVD), nonlinear phase accumulation through self-phase modulation (SPM), and some form of amplitude modulation from a saturable absorber. Fundamental to mode locking is the ability to control accumulated phase shifts due to GVD and SPM. To do this, some mode-locked lasers are designed with a dispersion map consisting of both negative and positive dispersion segments [1]. The change in sign of the dispersion causes the dissipative dispersion-managed (DM) solitons to temporally broaden and recompress as they propagate. Similar to conservative DM solitons in fiber transmission [2], higher-energy pulses are possible owing to the increased average pulse duration [3,4]. Depending on the net average dispersion, two types of pulse evolution per map period are observed. For net-anomalous and slightly net-normal dispersion, the solitons stretch and compress twice per cavity round trip, reach a minimum duration in the middle of each segment, and acquire both signs of chirp. These pulse solutions have been referred to as stretched pulse (SP) solutions [3]. For larger net-normal dispersion values the solitons stretch and compress once, have minimum duration at the beginning of the normal dispersion segment, and are positively chirped throughout the cavity [4]. Here we will refer to this pulse evolution as positively chirped pulse (PCP) evolution. In this Letter, we describe families of dissipative DM solitons in a mode-locked fiber laser by using a distributed DM Ginzburg–Landau type equation. We highlight the main differences between dissipative DM solitons and their conservative DM counterparts. Both types of pulse evolution observed experimentally [3,4] are obtained and completely classified with a reduced system of ordinary differential equations.

Pulse propagation in a mode-locked fiber laser can be modeled with a normalized, distributed equation

$$iu_z + \frac{d(z)}{2}u_{tt} + \gamma|u|^2u = i\left[\frac{g_0}{1+\|u\|^2/e_0} - \frac{l_0}{1+|u|^2/p_s}\right]u, \tag{1}$$

where u represents the electric field envelope normalized by the peak field power P_0, $\|u\|^2=\int|u|^2\mathrm{d}t$ is the energy of the pulse, t represents time in the rest frame of the pulse normalized by T_0, and z is the propagation distance normalized by the cavity length L. The normalized GVD and SPM coefficients are given by $d(z)=-\beta_2(z)L/T_0^2$ and $\gamma=2\pi n_2P_0L/(\lambda_0A_{\mathrm{eff}})$, respectively. Here β_2 is the fiber dispersion coefficient, n_2 is the nonlinear refractive index, λ_0 is the carrier wavelength, and A_{eff} is the effective fiber area. Equation (1) differs from the well-known nonlinear Schrödinger equation (NLSE) owing to the dissipative terms on the right-hand side of the equation, which represent gain saturation and an ideal saturable absorber [1]. The dissipative parameters $g_0=LG$, $e_0=E_{\mathrm{sat}}/(P_0T_0)$, $l_0=L\Gamma$, and $p_s=P_{\mathrm{sat}}/P_0$ are the normalized small-signal gain coefficient, saturation energy, unsaturated loss coefficient, and saturation power, respectively. Here G (in inverse meters) is the linear gain from amplification, Γ (in inverse meters) is the distributed losses in the cavity, E_{sat} (in nanojoules) is the saturation energy of the gain medium, and P_{sat} (in milliwatts) is the saturation power for the saturable absorber. In contrast to prior analysis of Eq. (1) [5], here we characterize the intramap dynamics and classify the different families of dissipative DM solitons.

To illustrate the possible pulse solutions and dynamics, we consider a simple two-step dispersion map so that $d(z)=d+\bar{d}$ for $(N-1)L<z<NL$ and $d(z)=-d+\bar{d}$ for $NL<z<(N+1)L$, where $d(>0)$ is the map depth and $\bar{d}$ is the average dispersion value. The dissipative terms in Eq. (1) play an important role in the scalings considered and are responsible for major differences between properties of DM solitons in laser

0146-9592/09/213286-3/$15.00

systems and in fiber transmission lines. The energy saturation determines the pulse power P_0, allowing us to choose the appropriate pulse duration T_0 to scale the ratio of the SPM coefficient γ to the dispersion coefficient d [6]. In all simulations, we let the ratio of the normalized SPM to GVD coefficient $\gamma/d=1$.

Numerical simulations of Eq. (1) with a two-step dispersion map show that for a wide range of parameter space stable and robust pulse solutions exist. These solutions are similar to DM solitons in that they are periodic solutions that broaden and compress depending on their position within the dispersion map. In contrast to the conservative DM solitons, however, the periodic breathers act as stable attractors to the system. From the final periodic state, the minimum pulse duration $\tau_{\min}$ and maximum energy $E_{\max}$ within each map period can be calculated. Figure 1 shows solution branches that are characterized by the dispersion ratios $\Delta=\bar{d}/d$. Each data point corresponds to a numerical simulation of Eq. (1) with a two-step dispersion map in which a stable breathing evolution is the final state. The solutions are classified in terms of the maximum energy $E_{\max}$ and the map strength $S=2dL/\tau_{\min}^2$, which is typically used to classify DM systems [7].

Figure 1 illuminates distinct differences with conservative DM solitons [7]. For DM solitons with dispersion ratios $\Delta\ (=)>0$, the map strength correlates to the map depth [7]. In contrast, dissipative DM solitons in this regime exist only at high map strengths regardless of map depth. At low map depths, the gain/loss saturation provides the necessary stabilization to achieve high-power, ultrashort pulses [see Fig. 2(b)]. DM solitons with dispersion ratio $\Delta\ (=)<0$ exist only for large map depths [7,8]. In contrast, dissipative DM solitons exist for both small and large map depths. It is interesting that these branches are discontinuous. For example, for the ratio $\Delta=-0.01$, there exist three branches, in the top right, bottom

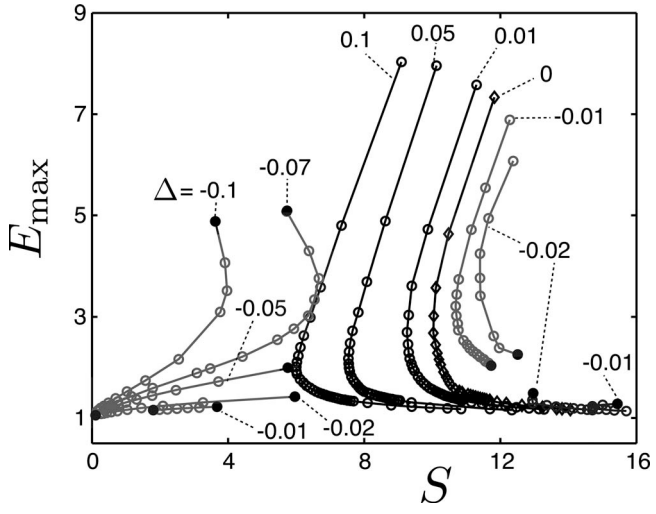

Fig. 1. Dependence of maximum pulse energy on map strength for a range of average cavity dispersion values $\Delta=\bar{d}/d$. Each point represents a stationary solution of Eq. (1) with a two-step map for $L=1$. Dissipative parameters are $g_0=2$, $e_0=1$, $l_0=1$, and $p_s=3$.

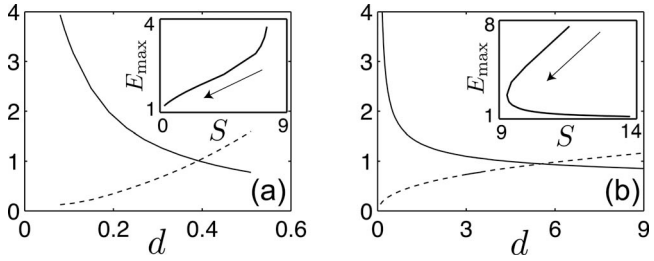

Fig. 2. Trends of the pulse amplitude (solid) and duration (dashed) along two distinct branches (insets) for (a) $\Delta=-0.05$, (b) $\Delta=0.01$.

right, and bottom left of Fig. 1. The corresponding map depths for these branches are $d\in(0.1,0.32)$ (top right), $d\in(0.33,1.23)$ (bottom left), and $d\in(3.5,13)$ (bottom right). Only the bottom right branch, where the map depth d is large, has a counterpart in the conservative NLSE system [7]. Further, for $\Delta<0$ there exist new solution branches that stem from the point $(S,E_{\max})=(0,1)$. We emphasis that the $\Delta<0$ branches terminate at the solid dots and cannot be extended numerically. Figure 2 shows the typical trends of the pulse amplitude and duration along examples of each type of branch. Following the solution branch along the direction of the arrow (inset) corresponds to increasing map depth d (and net dispersion). For both branches, at small net dispersion, the amplitude is large, while the pulse duration is small, leading to high-energy pulses. As the map depth is increased, the amplitude decreases, while the pulse duration increases until the energy approaches a constant value.

In Fig. 1, the solutions along the branches stemming from the point $(S,E_{\max})=(16,1)$ (and to their right) have a SP evolution that is similar to typical DM solitons of the conservative NLSE. Along the branches that stem from the point $(S,E_{\max})=(0,1)$ the intramap pulse evolution is clearly distinct and of PCP type. In general these pulses exist for large net-normal dispersion and are broad and highly chirped. These solutions have recently been achieved experimentally [4]; however, in that particular laser there is no nonlinearity in the anomalous dispersion segment, making Eq. (1) an approximate model. To gain insight into the different pulse evolutions, we apply the variational method [9] with pulse ansatz [8]

$$u(t,z)=\sqrt{\eta(z)}\,\exp[-(t/\tau(z))^2+iC(z)t^2+i\varphi(z)]. \quad (2)$$

The peak intensity (η), pulse duration (τ), and chirp parameter (C) satisfy the ordinary differential equations

$$\eta_z=-2\,d(z)C\eta+\left[\frac{2g_0e_0}{c_1e_0+\eta\tau}-l_0(3F_0-4F_2)\right]c_1\eta, \quad (3a)$$

$$\tau_z=2d(z)C\tau-l_0(4F_2-F_0)c_1\tau, \quad (3b)$$

$$C_z = 2d(z)\left[\frac{1}{\tau^4} - C^2\right] - \frac{\sqrt{2}}{2}\gamma\frac{\eta}{\tau^2}, \tag{3c}$$

where $F_j = \int_{-\infty}^{\infty} t^j f^2(t)/[1+\eta/p_s f^2(t)]\mathrm{d}t$, $f(t) = \exp(-t^2)$, and $c_1 = \sqrt{2/\pi}$. The functions $3F_0 - 4F_2$ and $4F_2 - F_0$ can easily be calculated as a function of η/p_s and are positive. A comparison between the final solution state of the reduced model (2) and the full evolution equation (1) is shown in Fig. 3 over two map periods. Although the reduced model is constrained by the ansatz assumption, it is remarkable how accurately it models the full equation dynamics.

Numerical simulations suggest when the dissipative DM soliton reaches its stable periodic evolution, the main pulse shaping is dominated by GVD and SPM, with the dissipative processes retreating to a secondary role. Neglecting the dissipative terms in Eqs. (3), we are able to solve Eqs. (3a) and (3b) in terms of the accumulated chirp $\int_0^z \mathrm{d}(s)C(s)\mathrm{d}s$. Using these solutions and setting Eq. (3c) to zero gives the necessary condition

$$\int_0^z C(s)\mathrm{d}s < -\frac{\log(\tau_0^4 C^2)}{8d(1+\Delta)} \tag{4}$$

for C to have a turning point in the anomalous dispersion segment, where (η_0, τ_0, C_0) are the solution parameters at the beginning of the anomalous segment. Equation (4) provides a key insight into the pulse evolution. For example, in Fig. 3 at the point $z = \bar{z}$ the chirp and accumulated chirp are roughly the same for both SP and PCP evolutions. However, at this point inequality (4) is satisfied for SP evolution,

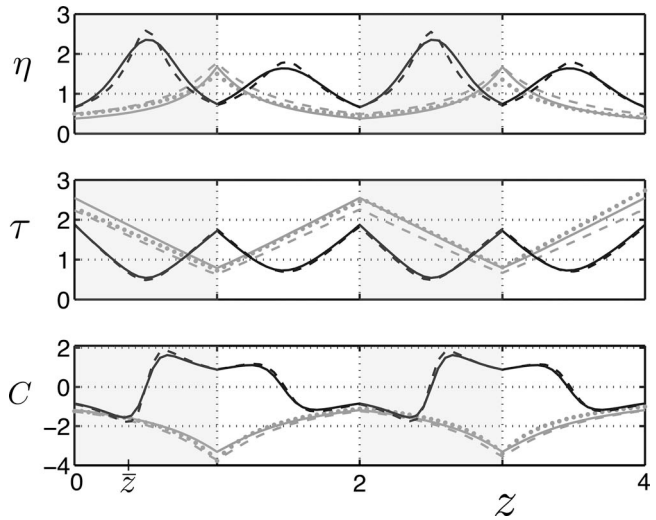

Fig. 3. Evolution of pulse parameters for typical SP (black) and PCP (gray) solutions from both reduced model (3) (dashed) and full model (1) (solid). Also included is analytic solution (5) (gray dots). Dissipative parameters are the same as in Fig. 1, and map parameters are $d=1$, $\bar{d}=0.01$ (SP), and $d=0.3$, $\bar{d}=-0.015$ (PCP). Shaded regions correspond to the anomalous GVD segment.

where it is not satisfied for the PCP evolution owing to its large initial duration τ_0 and smaller value of $d(1+\Delta)$. Indeed, inequality (4) is not satisfied anywhere within the anomalous segment for the PCP evolution, and the turning point for the chirp is when the dispersion changes signs. For broad PCP solutions, approximate solutions to Eqs. (3) can be obtained. Neglecting both the dissipative terms as well as $O(1/\tau^2)$ terms, Eqs. (3) have the solutions

$$\eta(z) = \frac{\eta_0}{1 + 2d(\pm 1 + \Delta)C_0 z}, \tag{5a}$$

$$\tau(z) = \tau_0(1 + 2d(\pm 1 + \Delta)C_0 z), \tag{5b}$$

$$C(z) = \frac{C_0}{1 + 2d(\pm 1 + \Delta)C_0 z}, \tag{5c}$$

where since $C_0 < 0$, $z < (2d(1+\Delta)|C_0|)^{-1}$ in the anomalous dispersion segment. These analytic solutions are plotted in Fig. 3 (gray dots) and show excellent agreement with both solutions to the reduced model (3) and simulations of the full equation (1). In deriving Eqs. (5), the nonlinearity has been neglected. Thus the PCP evolution is governed mainly by linear processes, although the stabilization of such solutions requires nonlinearity and gain/loss saturation. Future work will investigate the detailed relation between the dynamics of Eq. (1) and that observed in [4].

In conclusion, we have extended dispersion-managed (DM) soliton theory to dissipative DM solitons that are characterized by the average dispersion, map strength, and energy. Both stretched pulse and positively chirped pulse evolutions are observed and characterized by a simple inequality. In the case of positively chirped pulses, semianalytic solutions are obtained.

References

1. H. Haus, IEEE J. Sel. Top. Quantum Electron. **6**, 1173 (2000).
2. S. K. Turitsyn, E. G. Shapiro, S. B. Medvedev, M. P. Fedoruk, and V. K. Mezentsev, C. R. Phys. **4**, 145 (2003).
3. K. Tamura, E. P. Ippen, H. A. Haus, and L. E. Nelson, Opt. Lett. **18**, 1080 (1993).
4. F. O. Ilday, J. R. Buckley, W. G. Clark, and F. Wise, Phys. Rev. Lett. **92**, 213902 (2004).
5. M. J. Ablowitz, T. P. Horikis, and B. Ilan, Phys. Rev. A **77**, 033814 (2008).
6. Y. Chen, F. X. Kärtner, U. Morgner, S. H. Cho, H. A. Haus, E. P. Ippen, and J. G. Fujimoto, J. Opt. Soc. Am. B **16**, 1999 (1999).
7. N. J. Smith, N. J. Doran, F. M. Knox, and W. Forysiak, Opt. Lett. **21**, 1981 (1996).
8. J. N. Kutz and S. G. Egangelides, Opt. Lett. **23**, 685 (1998).
9. A. Bondeson, M. Lisak, and D. Anderson, Phys. Scr. **20**, 479 (1979).